Vol. 23 • No. 14 • April 12 • 2011

D10488

www.advmat.de

ADVANCED MATERIALS

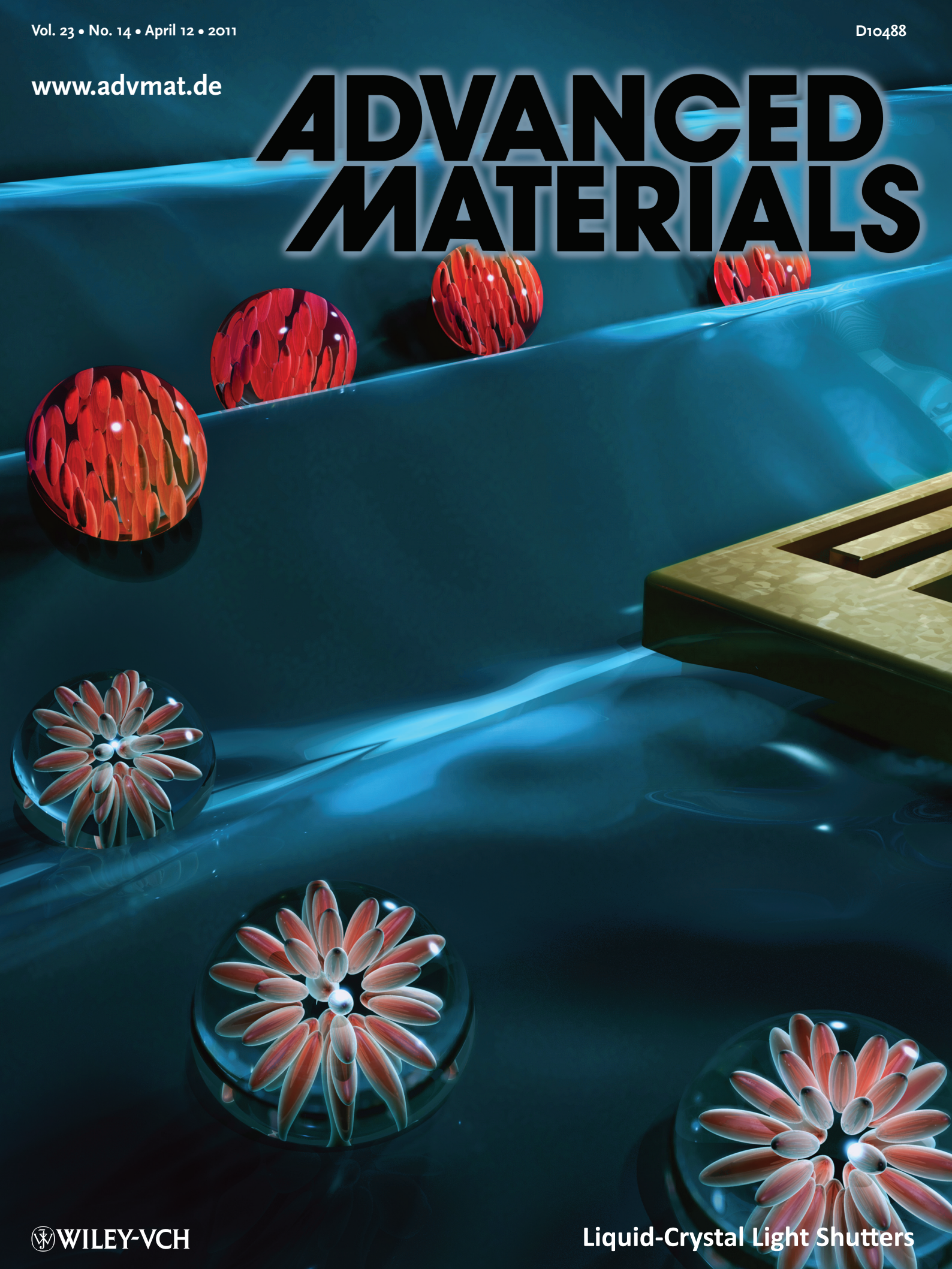

WILEY-VCH

Liquid-Crystal Light Shutters

Surface Acoustic Wave Driven Light Shutters Using Polymer-Dispersed Liquid Crystals

*Yan Jun Liu, Xiaoyun Ding, Sz-Chin Steven Lin, Jinjie Shi, I-Kao Chiang, and Tony Jun Huang**

In recent years, polymer-dispersed liquid crystals (PDLCs)[1] have been used in many applications including smart windows,[2] displays,[3] microlenses,[4,5] lasers,[6,7] and data storage,[8] due to their excellent electro-optical properties. PDLC films can be prepared between two conductive, transparent substrates using methods such as encapsulation, thermally induced phase separation, solvent-induced phase separation, and polymerization-induced phase separation.[9] Within a PDLC film, liquid crystals (LCs) are generally trapped in a transparent polymer medium, thus forming micrometer-scale LC droplets. The random dispersion of LC droplets in the polymer matrix causes a strong scattering of light due to the significant refractive index mismatch between the two materials; therefore, a PDLC film is naturally opaque. Based on laser interference holography, various periodic structures such as gratings[10–12] and photonic crystals,[13,14] can be also introduced inside the film, coined as holographic PDLCs (HPDLCs).[15] The application of an electric field can re-orientate the LC molecules inside a droplet, thus modulating the refractive index difference between the polymer matrix and the LC. A complete refractive index match between the two materials can be achieved by tuning the LCs to a specific orientation. In such a way, the PDLC film can be switched from opaque to transparent. The switching properties of PDLCs are influenced by many variables including the size and shape of the LC droplets,[16,17] and molecular interactions between the LCs and polymer matrix.[18,19]

The dynamic switching of PDLCs has been extensively studied based on electrically- and optically-driven methods;[20,21] however, both methods have their respective limitations. For instance, electrically-driven PDLCs require a high driving electric field (>1 V/μm),[18] while optically-driven methods have shown poor optical contrast (only 1–3).[20] To overcome these limitations, researchers continue to search for driving schemes that can achieve low power consumption, high throughput, and excellent optical properties.

Dr. Y. J. Liu, X. Ding, S.-C. S. Lin, Dr. J. Shi, I.-K. Chiang, Prof. T. J. Huang
Department of Engineering Science and Mechanics
The Pennsylvania State University
University Park, PA 16802, USA
Email: junhuang@psu.edu
Dr. J. Shi
The DOW Chemical Company
Spring House Technology Center
Spring House, PA 19477, USA

DOI: 10.1002/adma.201003708

Besides electrical and optical driving, LC re-alignment has also been demonstrated based on the acousto-optic effect,[22–24] where acoustic waves change the optical axis of a LC system, thus changing the transmitted light intensity.[23] Various mechanisms have been proposed to explain the LC molecules' re-orientation upon application of acoustic waves, such as acoustic streaming[25,26] and minimum entropy generation.[27] Acoustic streaming describes a steady flow in a fluid generated by propagating acoustic waves.[28] Due to the absorption, viscosity, and thermal conduction of the fluid, the acoustic wave attenuates while propagating. The attenuated acoustic wave exerts a net force on the fluid through momentum conservation and causes the steady flow. Ozaki *et al*. used acoustic streaming to change the alignment of cholesteric LC molecules[29] and demonstrated a lasing effect.[30] LC realignment based on the acousto-optic effect has already found valuable applications including imaging[31,32] and medical diagnostics.[33] In most LC-based acousto-optic devices, bulk acoustic waves (BAWs) have been employed. In general, BAWs have larger power consumption than surface acoustic waves (SAWs) – a sound wave that propagates along the surface of an elastic material. In addition, BAW systems are not compatible with existing fast-prototyping techniques (e.g., soft lithography), limiting device miniaturization. As such, SAWs are more desirable for many device settings due to their unique characteristics: 1) most of their energy is confined within one to two wavelengths normal to the surface,[34] making them energy-efficient when manipulating the contact materials; 2) SAW-based devices are free of contamination, only introducing low-power mechanical vibrations to the system. Recently, researchers have demonstrated microfluidic devices utilizing SAW-based mixing,[35] pumping,[36] concentration,[37] particle focusing,[38] and tweezers.[39]

In this Communication, we demonstrate a SAW-driven PDLC light shutter by integrating a cured PDLC film and a pair of interdigital transducers (IDTs) onto a piezoelectric substrate. The IDTs were used to generate the SAW for driving the PDLC film. **Figure 1** illustrates the layout and working principle of the SAW-driven PDLC light shutter. A PDLC cell is located in between two identical IDTs, which are deposited on a piezoelectric substrate with a parallel arrangement. One IDT is used for SAW generation and the other is used for SAW detection. A radio-frequency (RF) signal is applied to a single IDT to generate a SAW, which propagates along the surface of the piezoelectric substrate (*x*-direction in Figure 1). By tuning the applied frequencies from the function generator and monitoring the frequency-dependent output voltage from the detection IDT that is connected to an oscilloscope, an optimal resonant frequency can be selected for the driving frequency. At

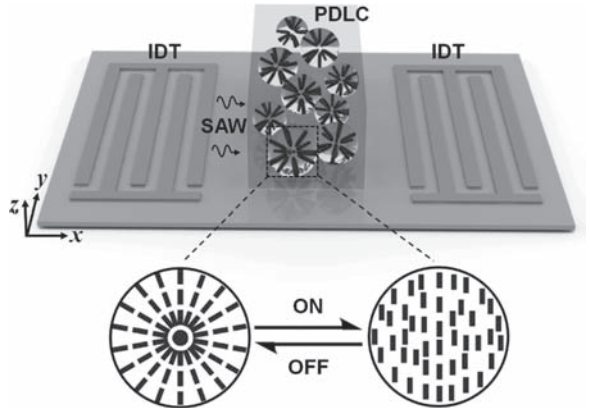

Figure 1. The device structure and working principle for the SAW-driven PDLC light shutter. The magnified part shows a reversible switching process between two different LC droplet configurations.

this working frequency, the acousto-optic properties of PDLCs will be investigated.

When the propagating SAW encounters the PDLCs, a longitudinal wave is induced and leaks into the PDLCs. The sample's temperature increases as the longitudinal wave attenuates, causing a thermal effect in the sample. Both the viscosity and the birefringence of the LCs decrease with the increase in temperature. The longitudinal-mode leakage wave also causes pressure fluctuations and induces a streaming effect in the LC-rich regions. In a pure nematic LC medium, this kind of acoustic streaming causes a vortical flow across the LC cell that is responsible for re-orientating the LC molecules perpendicular to the substrate.[26] We believe that this acoustic wave-induced shear-flow uses a similar mechanism to re-orientate the LC molecules inside the LC droplets in the PDLC sample. In our case, the SAW propagation is along *x*-axis and the PDLC film normal is along *z*-axis, as labeled in Figure 1. The induced tilt angle $\theta(x, z)$ of the LC director from the *z*-axis by the shear-flow can be described as:[25]

$$K_{33}\partial^2\theta/\partial z^2 + \kappa_1 \partial\langle v\rangle/\partial z = 0 \quad (1)$$

where K_{33} is Frank's bend elastic constant, κ_1 is Leslie's shear-torque coefficient, and $\langle v\rangle$ is the second-order velocity. When most of the LC molecules are realigned perpendicular to the substrate due to the flow-induced reorientation, the normally incident light only sees the ordinary refractive index of the LCs regardless of its polarization. In our experiments, we intentionally chose LCs with the ordinary refractive index close to the refractive index of the cured polymer. As a result, under SAW application the PDLC film becomes homogeneous and transparent. In contrast, without an applied SAW, the PDLC film causes strong scattering due to the refractive index mismatch between the polymer matrix and LC droplets, thus demonstrating a non-transparent state. This reversible switching process is shown in the magnified part of Figure 1.

In our experiments, we found the optimum working frequency to be 18.76 MHz after the PDLC film was introduced to the piezoelectric substrate. We investigated the changes in the PDLC morphologies at this frequency. **Figure 2** shows the evolution of the PDLC morphologies as a function of time at the applied power of 34 dBm for a sample with LC concentration of 70 wt%. Under two crossed polarizers, the initial LC state shows strong scattering due to the anisotropic properties of LCs (Figure 2a). Upon SAW application, the PDLC film transitions into transparency from one side (near the working IDT) to the other (far from the working IDT) (Figure 2b-2e). The PDLC film becomes completely transparent after approximately 100 seconds, corresponding to the dark state observed under two crossed polarizers (Figure 2f).

We found that upon applying a SAW, the temperature of PDLC sample increased and saturated at ~40 °C. This occurred when the PDLC sample became totally transparent, and indicated the presence of a thermal effect caused by the attenuation of the SAW during the propagation. The measured attenuation of the incident SAW through the PDLC cell was ~17.5 dBm in our experiment, implying that the PDLC sample absorbed nearly half of the applied SAW energy. The increase in temperature caused a decrease in both the birefringence[40] and viscosity of the LCs. However, the final temperature (40 °C) in our experiment was still well below the clearing point of the LCs; further investigation revealed that the nematic-isotropic transition of the LCs occurred between 55 and 59 °C. Therefore, the LCs maintained their nematic properties at ~40 °C, and the thermal effect was not the main factor contributing to the transparency of the PDLC sample. In addition to the heating effect, we also observed streaming in our experiments at high LC concentrations. We believe that the streaming effect plays a dominant role in this SAW-driven PDLC light shutter. Provided that the LC maintains its nematic state, the realignment of LC molecules is the only way to change the transparency of the PDLC film. In our experiments, the PDLC film became fully transparent, indicating an index match between the LC droplets and the surrounding polymers along the light propagation

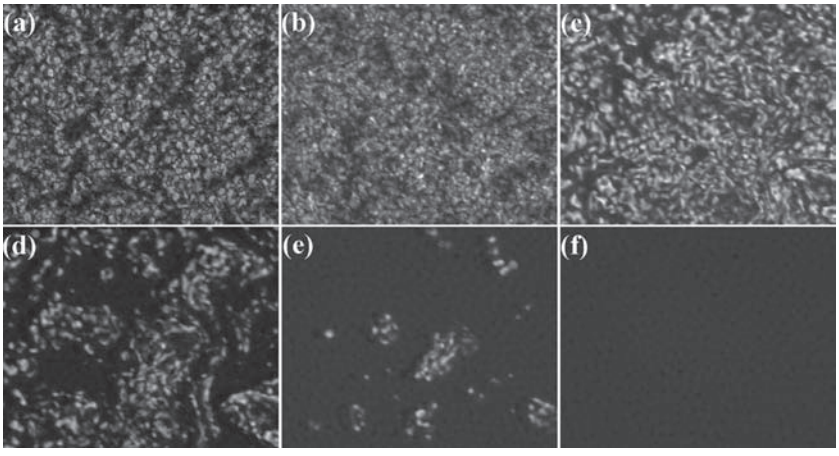

Figure 2. Observation of the optical microscopic PDLC morphology evolution with the application of acoustic power: (a) 0 second; (b) 20 seconds; (c) 40 seconds; (d) 60 seconds; (e) 80 seconds; (f) 100 seconds.

direction. Therefore, we concluded that the acoustic streaming re-oriented most of the LC molecules perpendicular to the substrate. To confirm this prediction, a control experiment was carried out, in which two identical RF signals were applied to both parallel IDTs simultaneously to drive the PDLC light shutter. In this case, the IDTs generated two counter-propagating SAWs that interfered to form a standing wave; no obvious streaming was observed in PDLCs with the total driving power applied to the sample held constant. If the thermal effect assumes the dominant role, we should observe the PDLC sample becoming transparent with extended driving time. However, we found no switching effect when the IDTs worked together, even with much longer time than the single IDT case. This indicates that acoustic streaming was the main cause for the switching of our PDLC shutter.

Furthermore, we explored the transmission dynamics of the PDLC sample by switching the SAW on and off. **Figure 3**a shows the transmission changes during the SAW on/off processes under different acoustic powers. It is clear that the switching-on process strongly depends on the acoustic power. The higher acoustic powers correlate to faster switching-on times and higher optical contrast ratios. However, the switching-on time and the contrast saturate at a certain acoustic power. The switching-off time depends only on the material properties of LCs and remains nearly constant. The optimized switching-on and switching-off times were ~14 and ~5 s, respectively, for an applied acoustic power of 36 dBm. The achieved optical contrast (defined as the ratio of the highest transmission to the lowest transmission) was ~33. It is worth mentioning here that the switching time and acoustic power can be further improved. A decrease in droplet size can significantly improve the switching-off time, as the switching-off time in PDLCs is proportional to r^2, where r is the radius of a LC droplet.[18] In general, big droplets induce slow switching time, but strong scattering; while small droplets lead to fast switching time, but weak scattering. The trade-off between the switching time and optical contrast demands a suitable droplet size to optimize performance. A PDLC film with uniform micron-sized droplets (1–3 μm) could have a switching time on the order of milliseconds.[41] In addition, adding a surfactant to PDLCs could effectively decrease the driving power because the surfactant forms an intermediate layer between the LC droplet and surrounding polymers, acting like a lubricant.[42] The insets I and II of Figure 3a show the OFF and ON states of a PDLC sample, respectively. When the acoustic power is off, the film is opaque (inset I of Figure 3a); and when the acoustic power is on, the film is transparent and the letters "PDLC" underneath the film become visible (inset II of Figure 3a). We also note that optical bounces are clearly observed immediately after turning off the SAW and during self-relaxation; this phenomenon is likely due to the backflow effect.[43,44] The backflow effect is a shear flow of LCs that causes temporary reverse rotation of the LC director in the middle of the cell after the SAW across the cell is removed. From Figure 3a, we can see that higher SAW power corresponds to more pronounced optical bounces, indicating a stronger backflow effect. Figure 3b shows a detailed examination of the switching-on process. The experimental curves were fitted using a double-exponential function:

$$I(t) = I_{min} + I_0 \sin^2 \times \left\{ \frac{1}{2}\delta_1 \left[1 - \exp\left(-t/\tau_1\right)\right] + \frac{1}{2}\delta_2 \left[1 - \exp\left(-t/\tau_2\right)\right] \right\} \quad (2)$$

where δ_i and τ_i ($i = 1, 2$) are the fitting parameters, representing phase retardation and switching-on time. Figure 3b shows the double-exponential function fits the dynamic switching behavior well over the full range of time; this observation implies that the switching process of the PDLC sample has different relaxation modes at different time scales.

In summary, we have demonstrated a SAW-driven PDLC light shutter based on the acoustic streaming-induced realignment of LC molecules as well as absorption-related thermal diffusion. The working mechanism was analyzed theoretically and the acousto-optical properties of the PDLC sample were characterized experimentally. This device shows excellent performance in terms of energy consumption and optical contrast, which is important for applications such as displays and smart windows. In addition, the IDTs fabricated by standard photolithography are highly compatible for future system integration. Our future work includes developing SAW-driven PDLC systems with faster response and lower energy consumption—this could be achieved by optimizing the mechanical and dielectric properties of PDLC (e.g., using less viscous ferroelectric LCs with higher birefringence, controlling the LC droplets size, and adding surfactants). We expect that with further developments, the SAW-based driving scheme could have significant impact on future PDLC-based nanophotonic and plasmonic devices.[45–52]

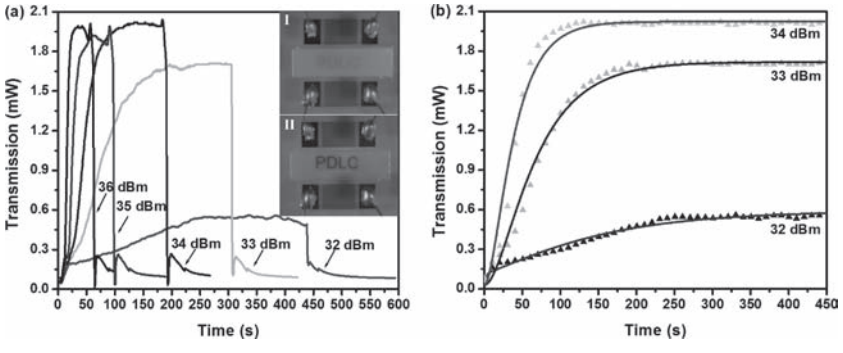

Figure 3. (a) Transmission changes during on and off processes under different acoustic power. The insets I and II show the imaging quality at the OFF and ON states of the device respectively. (b) The magnified switching-on process under different acoustic power. The triangular-dot curve shows the experimental data and the solid curve shows the theoretical fitting using a double-exponential function.

Acknowledgements

We gratefully acknowledge the help from Brian Kiraly in manuscript preparation and the financial support from Air Force Office of Scientific Research (AFOSR), National Science Foundation (NSF), and

the Penn State Center for Nanoscale Science (MRSEC). Components of this work were conducted at the Penn State node of the NSF-funded National Nanotechnology Infrastructure Network.

Received: October 8, 2010
Revised: November 24, 2010
Published online: March 14, 2011

[1] J. W. Doane, N. A. Vaz, B.-G. Wu, S. Zumer, *Appl. Phys. Lett.* **1986**, *48*, 269.
[2] D. Cupelli, F. P. Nicoletta, S. Manfredi, M. Vivacqua, P. Formoso, G. De Filpo, G. Chidichimo, *Sol. Energ. Mat. Sol. Cells* **2009**, *93*, 2008.
[3] C. D. Sheraw, L. Zhou, J. R. Huang, D. J. Gundlach, T. N. Jackson, M. G. Kane, I. G. Hill, M. S. Hammond, J. Campi, B. K. Greening, J. Francl, J. West, *Appl. Phys. Lett.* **2002**, *80*, 1088.
[4] H. Ren, Y.-H. Fan, Y.-H. Lin, S.-T. Wu, *Opt. Commun.* **2005**, *247*, 101.
[5] G.-R. Xiong, G. -Z. Han, C. Sun, H. Xu, H.-M. Wei, Z.-Z. Gu, *Adv. Funct. Mater.* **2009**, *19*, 1082.
[6] Y. J. Liu, X. W. Sun, H. I. Elim, W. Ji, *Appl. Phys. Lett.* **2006**, *89*, 011111.
[7] Y. J. Liu, X. W. Sun, H. I. Elim, W. Ji, *Appl. Phys. Lett.* **2007**, *90*, 011109.
[8] Y. J. Liu, X. W. Sun, *Appl. Phys. Lett.* **2007**, *90*, 191118.
[9] P. S. Drzaic, *Liquid crystal dispersions*, World Scientific, Singapore **1995**.
[10] R. L. Sutherland, L. V. Natarajan, V. P. Tondiglia, T. J. Bunning, *Chem. Mater.* **1993**, *5*, 1533.
[11] Y. J. Liu, B. Zhang, Y. Jia, K. S. Xu, *Opt. Commun.* **2003**, *218*, 27.
[12] Y. J. Liu, X. W. Sun, J. H. Liu, H. T. Dai, K. S. Xu, *Appl. Phys. Lett.* **2005**, *86*, 041115.
[13] V. P. Tondiglia, L. V. Natarajan, R. L. Sutherland, D. Tomlin, T. J. Bunning, *Adv. Mater.* **2002**, *14*, 187.
[14] Y. J. Liu, X. W. Sun, *Jpn. J. Appl. Phys.* **2007**, *46*, 6634.
[15] T. J. Bunning, L. V. Natarajan, V. P. Tondiglia, R. L. Sutherland, *Annu. Rev. Mater. Sci.* **2000**, *30*, 83.
[16] P. S. Drzaic, *Proc. SPIE* **1990**, *1257*, 29.
[17] G. P. Montgomery, J. L. West, W. Tamura-Lis, *J. Appl. Phys.* **1991**, *69*, 1605.
[18] B. -G. Wu, J. H. Erdmann, J. W. Doane, *Liq. Cryst.* **1989**, *5*, 1453.
[19] G. P. Montgomery, J. L. West, W. Tamura-Lis, *J. Appl. Phys.* **1991**, *69*, 1605.
[20] H. -K. Lee, A. Kanazawa, T. Shiono, T. Ikeda, T. Fujisawa, M. Aizawa, B. Lee, *J. Appl. Phys.* **1999**, *86*, 5927.
[21] Y. J. Liu, Y. B. Zheng, J. J. Shi, H. Huang, T. R. Walker, T. J. Huang, *Opt. Lett.* **2009**, *34*, 2351.
[22] J. V. Selinger, M. S. Spector, V. A. Greanya, B. T. Weslowski, D. K. Shenoy, R. Shashidhar, *Phys. Rev. E* **2002**, *66*, 051708.
[23] A. P. Malanoski, V. A. Greanya, B. T. Weslowski, M. S. Spector, J. V. Selinger, R. Shashidhar, *Phys. Rev. E* **2004**, *69*, 021705.
[24] V. A. Greanya, A. P. Malanoski, B. T. Weslowski, M. S. Spector, J. V. Selinger, *Liq. Cryst.* **2005**, *32*, 933.
[25] W. Helfrich, *Phys. Rev. Lett.* **1972**, *29*, 1583.
[26] K. Miyano, Y. R. Shen, *Phys. Rev. A* **1977**, *15*, 2471.
[27] J. L. Dion, A. D. Jacob, *Appl. Phys. Lett.* **1977**, *31*, 490.
[28] T. Frommelt, D. Gogel, M. Kostur, P. Talkner, P. Hanggi, A. Wixforth, *IEEE Trans. Ultrason., Ferroelectr., Freq. Control* **2008**, *55*, 2298.
[29] R. Ozaki, T. Shinpo, M. Ozaki, H. Moritake, *Jpn. J. Appl. Phys.* **2007**, *46*, L489.
[30] R. Ozaki, T. Shinpo, M. Ozaki, H. Moritake, *Jpn. J. Appl. Phys.* **2008**, *47*, 1363.
[31] D. W. Gerdt, M. C. Baruch, C. M. Adkins, *Proc. SPIE* **1999**, *3635*, 58.
[32] J. S. Sandhu, H. Wang, W. J. Popek, *Proc. SPIE* **2000**, *3955*, 94.
[33] J. S. Sandhu, R. A. Schmidt, P. J. La Riviere, *Med. Phys.* **2009**, *36*, 2324.
[34] C. Campbell, J. C. Burgess, *J. Acoust. Soc. Am.* **1991**, *89*, 1479.
[35] T. Frommelt, M. Kostur, M. Wenzel- Schafer, P. Talkner, P. Hanggi, A. Wixforth, *Phys. Rev. Lett.* **2008**, *100*, 034502.
[36] Z. Guttenberg, H. Muller, H. Habermuller, A. Geisbauer, J. Pipper, J. Felbel, M. Kielpinski, J. Scriba, A. Wixforth, *Lab Chip* **2005**, *5*, 308.
[37] M. K. Tan, J. R. Friend, L. Y. Yeo, *Lab Chip* **2007**, *7*, 618.
[38] J. Shi, X. Mao, D. Ahmed, A. Colletti, T. J. Huang, *Lab Chip* **2008**, *8*, 221.
[39] J. Shi, D. Ahmed, X. Mao, S.-C. S. Lin, A. Lawit, T. J. Huang, *Lab Chip* **2009**, *9*, 2890.
[40] S. T. Wu, *Phys. Rev. A* **1986**, *33*, 1270.
[41] Q. Meng, H. Cao, M. Kashima, H. Liu, H. Yang, *Liq. Cryst.* **2010**, *37*, 189.
[42] Y. J. Liu, X. W. Sun, H. T. Dai, J. H. Liu, K. S. Xu, *Opt. Mater.* **2005**, *27*, 1451.
[43] C. Z. van Doorn, *J. Appl. Phys.* **1975**, *46*, 3738.
[44] D. W. Berreman, *J. Appl. Phys.* **1975**, *46*, 3746.
[45] Z. Liu, Q. H. Wei, X. Zhang, *Nano. Lett.* **2005**, *5*, 957.
[46] Y. Xiong, Z. Liu, S. Durant, H. Lee, C. Sun, X. Zhang, *Opt. Express* **2007**, *15*, 7095.
[47] V. K. S. Hsiao, Y. B. Zheng, B. K. Juluri, T. J. Huang, *Adv. Mater.* **2008**, *20*, 3528.
[48] C. Novo, A. M. Funston, P. Mulvaney, *Nature Nanotech.*, **2008**, *3*, 598.
[49] Y. J. Liu, T. J. Huang, H. T. Dai, X. W. Sun, *Opt. Express* **2009**, *17*, 12418.
[50] Y. J. Liu, Q. Z. Hao, J. S. T. Smalley, J. Liou, I. C. Khoo, T. J. Huang, *Appl. Phys. Lett.* **2010**, *97*, 091101.
[51] L. Feng, Z. Liu, V. Lomakin, Y. Fainman, *Appl. Phys. Lett.* **2010**, *96*, 041112.
[52] C. Ruppert, J. Neumann, J. B. Kinzel, H. J. Krenner, A. Wixforth, M. Betz, *Phys. Rev. B* **2010**, *82*, 081416(R).